New developments around the Butterfly antenna

Didier Charrier

Subatech, École des Mines de Nantes - CNRS/IN2P3 - Université de Nantes, France

Abstract. The Butterfly antenna is a compact, active and dual polarization ultra wide band antenna initially designed in 2008 for the radio detection of extensive air showers in the [15-200] MHz frequency range. Butterfly antennas are in operations at Nançay for the CODALEMA experiment since October 2008, and at Auger for the AERA experiment since may 2013. Because of its good characteristics, the Butterfly antenna or its only associated LNA has been chosen by many other cosmic ray (TREND, HELYCON, COMPACT ARRAY) or radio astronomy experiments(NenuFAR). The design features of the Butterfly antenna will be explained in this paper with an emphasis on new developments as, an accurate noise model, a time domain impulse isotropy pattern and a new custom LNA named LONAMOS designed to improve the Butterfly characteristics.

Keywords: antenna, UWB, impulse response, LNA, noise matching, CODALEMA
PACS: <Replace this text with PACS numbers; choose from this list: `http://www.aip..org/pacs/index.html`>

INTRODUCTION

The Butterfly antenna [1] is an active dual polarization antenna designed and developed in 2008 to detect impulse electric fields generated by ultra high energy cosmic rays (UHECR) at first on the CODALEMA [2] experiment. Due to the impulse nature of the electromagnetic field, both an ultra wide band (UWB) and a low phase distortion are required. We need an high enough sensitivity to detect very weak impulse emerging from galactic background noise. Due to the high level of RFI that may occur in the SW and FM band, an high linearity is also required to avoid the production of unwanted intermodulation products in the clean band ranging from 15 MHz to 88 MHz and from 108 MHz to beyond. We also require an antenna radiating element with a low gain[3] to minimize the anisotropy.

ANTENNA RADIATING ELEMENT

On an ultra wide band, choosing a dipole like antenna as radiating element is not the easiest way to perform a power matching between the antenna impedance Z_{ant} and the input impedance of the LNA. Indeed, both the antenna radiation resistance R_{rad} and the reactance X_{ant} change strongly with the frequency as shown on Fig. 2.The LNA input impedance should be perfectly matched to the transmission line connecting a BALUN located at the antenne feedpoint to avoid multiple impulse bounces along it. We overcome this issue with the active antenna concept by placing the LNA at the antenna feedpoint. By removing the transmission line, power matching constraints becomes unnecessary. For the Butterfly antenna, we chose [1] an isosceles triangle shape(bowtie [3]) as radiating element. The base of the triangle is 0.84 m and its height is 1 m. The bowtie is a trade off between lowering both the Q-factor and the phase distortion, and both minimizing the weight and complexity of the radiator. The radiator half perimeter is 1.56 m resulting in a resonance frequency around 48 MHz maximizing the signal to noise ratio S/N around it. The 1.5 m antenna height above the actual soil which acts as an imperfect reflector, is a trade off between minimizing the antenna ground losses [3] and minimizing the antenna anisotropy at high frequencies.

THE ACTIVE ANTENNA SENSITIVITY

We can characterize the sensitivity of the butterfly antenna by a signal to noise ratio S_{out}/N_{out} at the LNA output. The signal is an impulse generated at the LNA output when the antenna radiator is receiving an impulse electric field induced by an UHECR. Three types of uncorrelated noises contribute to the total noise, the galactic background temperature, the antenna losses, and the LNA noise. Nevertheless we will consider the galactic temperature as a signal in the 20-80 MHz range: monitoring the galactic noise level allow to check accurately one antenna; It can also be used as a cross calibration signal on an antenna array. Thus the contribution of both the LNA noise and antenna losses

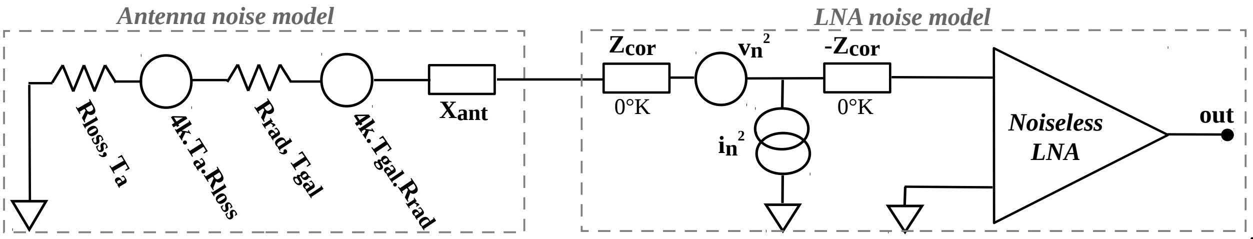

FIGURE 1. Noise equivalent circuit of the antenna and the LNA. The antenna impedance is composed of its reactance X_{ant}, its radiation resistance R_{rad} and its loss resistance R_{loss}. A Rothe and Dahlke [4] noise model is used tu fully model the LNA noise: uncoralated voltage v_n^2 and current i_n^2 noise sources and a 0 K correlation impedance Z_{cor}.

should be ideally 10 dB lower than the minimum galactic temperature contribution. As shown on Fig. 1, we model the galactic noise by the thermal noise of the antenna radiation resistance R_{rad} to the galactic temperature T_{gal}. Similarly we model the antenna losses by the thermal noise of a loss resistance R_{loss} to the room temperature T_a (290 K). In our frequency range, this noise is widely due to ohmic and dielectric losses occurring in the soil. In this paper, we model a typical average soil by setting its relative permittivity ε_r and its conductivity σ respectively to 13 and 5 mS.m^{-1}. From the electrical ground parameters and the antenna geometry, we extract by a NEC2 simulation both the equivalent loss resistance and the radiation resistance. With the galactic temperature data, we calculate the signal to noise ratio of the antenna radiating elements with $S/N|_{ant} = (T_{gal}.R_{rad})/(T_a R_{loss})$. It gives an absolute ceil limit to the S_{out}/N_{out} and is intrinsic to the antenna radiator including the ground plane. With the Butterfly antenna, $S/N|_{ant}$ is monotonically decreasing with the frequency and we obtain 10 dB at 90 MHz and 2 dB less for a desert type ground with σ=1 mS.m^{-1} and ε_r=5.5. We measure the LNA noise and fully model it on Fig. 1 by the 4 parameters of a T-type Rothe and Dahlke noise model[4]. We have uncorrelated voltage and current noise sources and a noiseless correlation impedance Z_{cor} composed of its correlation resistance R_{cor} set to 0 K and its correlation reactance X_{cor}. From the noise equivalent circuit of the active antenna on Fig. 1, we calculate the Signal to Noise ratio at the LNA output (Eq.1). We assume an antenna loss resistance proportional to its radiation resistance by a factor depending only on the antenna efficiency [3] η. So R_{loss} does not appear in Eq. 1.

$$\frac{S_{out}}{N_{out}} = \frac{\frac{T_{gal}}{T_a} R_{rad}}{\left(\frac{1-\eta}{\eta}\right) R_{rad} + r_n + g_n \left[\left(\frac{R_{rad}}{\eta} + R_{cor}\right)^2 + (X_{ant} + X_{cor})^2\right]} \quad with \;\; r_n = \frac{v_n^2}{4kT_a} \;\; and \;\; g_n = \frac{i_n^2}{4kT_a} \tag{1}$$

The simulated antenna parameters (R_{rad}, X_{ant}, η) and measured LNA parameters(r_n, g_n, R_{cor}, X_{cor}) depend respectively on the antenna radiator geometry and on the LNA architecture and input transistors. By design choice on both the antenna radiator and the LNA, we manage to obtain a S_{out}/N_{out} higher than 10 dB in the 20-80 MHz range and maximised beyond. For a given antenna, we see From Eq. 1 that it is worth designing a LNA with a low current noise. For a given LNA, we calculate(Eq.2) from Eq.1 the optimum values of R_{rad} and X_{ant} maximizing the S_{out}/N_{out} ratio.

$$R_{rad}^{opt} = \eta \sqrt{R_{cor}^2 + \frac{r_n}{g_n}}\,, \qquad X_{ant}^{opt} = -X_{cor} \tag{2}$$

The adjustment of R_{rad} to R_{rad}^{opt} and X_{ant} to X_{ant}^{opt} is the noise matching [4] of the antenna to the LNA. Note that we calculate exactly the same optimum antenna impedance minimizing the LNA noise factor [4] for a complex source impedance to room temperature. As we get rid of the power matching constraint, noise matching becomes a reachable target. But it is necessary only for frequencies where the S_{out}/N_{out} is lower than 10 dB. For the Butterfly antenna radiator with the new LNA named LONAMOS, we see on Fig. 2 that the simulated values of the antenna impedance are oscillating around their optimum values. The amplitude of the R_{rad} and X_{ant} oscillation is lowered by increasing the dipole thickness[3]. It explains why we chose a bowtie shape instead of a simple thin dipole shape as radiator for the Butterfly antenna. It would have been even better with a volumic conic shape but to the cost of the complexity and radiator weight. For a given antenna-LNA, adding a passive network array between the antenna and the LNA is another way to improve the noise matching. Fig. 2 shows the improvement in the 18-45 MHz range by adding a 2 μH inductor L parallel to the LNA input. Moreover it acts as a shunt at low frequencies attenuating the RFI power below 15 MHz. Finally we obtain on Fig. 2 a S_{out}/N_{out} higher than 10 dB in the 22-75 MHz range with the Butterfly-

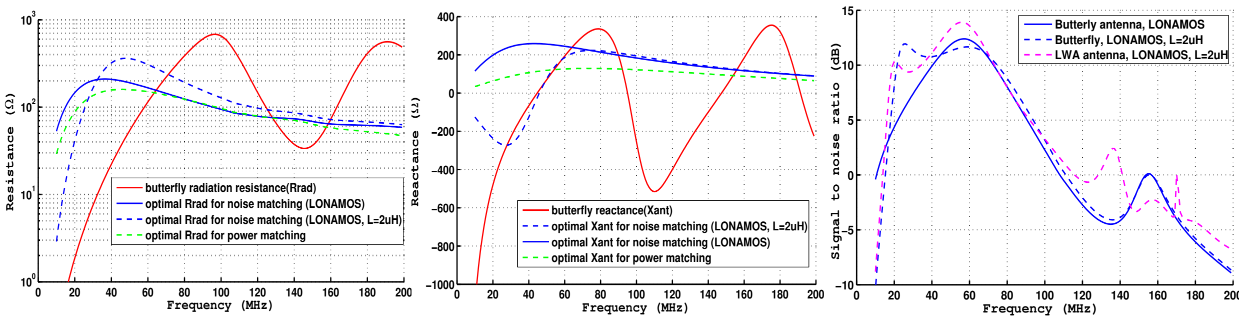

FIGURE 2. Noise characteristics: the left figure compare the simulated radiation resistance of the Butterfly antenna impedance to the optimum resistance required by the LONAMOS LNA to perform the noise matching. The middle figure is similarly the same but for the imaginary part. The right figure is the calculation of S/N at the LNA output for the Butterfly and LWA antennas.

LONAMOS (with L). We have similar results with the LWA antenna radiator [5] and LONAMOS (with L). Note that with LONAMOS, noise and power matching conditions are closed. The equivalent noise temperature of LONAMOS calculated at the LNA input with the butterfly impedance as source is ranging from 52 K to 144 K below 100 MHz and reach 200 K at 190 MHz.

LNA AND LINEARITY

The linearity of the active antenna depends only on its LNA. The LONAMOS LNA was designed and developed in 2011 to equip the butterfly antenna radiator. In order to lower the unwanted intermodulation products in a high level RFI environment, the main feature improvements compared to the previous CODALAMP [1] LNA, are an increase of the input compression point (ICP) and the input third order intercept point (IIP3). Other goals are the decrease of the LNA gain drift with the temperature and the characteristics uncertainties. LONAMOS is a two stages LNA with a fully differential architecture rejecting both even order harmonics and common mode noises. An high linearity is obtained thanks to an high open loop gain, a wide output stage dynamic range and a resistive feedback. LONAMOS is an application specific integrated circuit(ASIC). The ASIC technology allow a full custom design of each transistor of the chip. Thus the LNA can be deeply optimized to the antenna, which would be more difficult with a discrete SMD realization. We chose a 0.35 μm C35B4C3 technology from the AMS foundry offering only CMOS transistor in spite they comparatively have a lower transconductance than bipolar ones. But CMOS technology are cheap since widely used for digital circuits. The LNA input impedance can be digitally adjusted in order to optimize its noise features to other kinds of antennas. The default equivalent input impedance is closed to a 285 Ω resistance parallel to a 6 pF parasitic capacitance. We measured the characteristics and the scattering parameters of 160 LONAMOS and 146 CODALAMP, see Tab. 1: the standard deviations σ of characteristics uncertainties are roughly tree times less with the new LNA: we measure $\sigma(|S_{21}|)$=67 mdB, $\sigma(-\partial(\arg(S_{21}))/\partial\omega)$=54 ps, $\sigma(|S_{11}|)$=26 mdB.

TABLE 1. LNAs measured characteristics summary at 50 MHz(20 MHz for OCP and OIP3), for LNA nominal settings.

	OCP	OIP_3	G_P ; G_V	NF^* ; NF_{min}	$\Gamma_{in}(50\ \Omega)$	f_c	G_P drift	$P_{diss.}$
LONAMOS	15 dBm	33 dBm	26.8 ; 19.3 dB	0.8 ; 0.7 dB	0.69 - j0.13	>200 MHz	-4 mdB/K	340 mW
CODALAMP	0 dBm	14 dBm	33.7 ; 26 dB		0.74 - j0.1	>200 MHz	-26 mdB/K	310 mW

* for a power matched source impedance

TIME DOMAIN IMPULSE ISOTROPY PATTERN

In NEC2, we model a Butterfly antenna centred on the z-axis of a Cartesian coordinate system. The antenna height is placed 1.5 m above an XY lossy ground plane with one dipole aligned on the x-axis and the other on the y-axis. We use a spherical coordinate system with θ the zenith angle counted from the z-axis and φ the azimuth angle counted anticlockwise from the x-axis. We define a vector equivalent length $\vec{H}^{bfy}$ of the Butterfly antenna as the ratio of the voltage V_{out} developed at the LNA output to the complex value of an incoming electric field $\vec{E}(r,\theta,\varphi,\omega)$. This field has no radial component since we assume the far field radiation conditions [3]. $\vec{H}^{bfy}$ is the product of two factors. The first is the antenna vector effective height $\vec{H}^{ant}$ [3] defined as the ratio of the voltage V_{oc} developed at its opened terminal point to the incoming field. The second factor is the transfer function defined as the ratio of V_{out} and V_{oc} calculated from the simulated value of Z_{ant} and the S-parameters measured values of the LNA (with L=2 μH). In NEC2, we place a current sine source with an amplitude I_t at an emitting antenna feedpoint, perform a frequency sweep simulation and get the vector data of the induced electric field $\vec{E}$ for the distance r. From Eq. 3, we deduce $\vec{H}^{ant}$ of this transmitting antenna which is the same in receiving mode since the antenna radiator is passive. Note that NEC2 gives not directly $\vec{E}$ but a potential $\vec{V}^{nec}$ as defined in Eq. 4. Finally, we infer the calculation of the vector equivalent length $\vec{H}^{bfy}$ in Eq. 4, valid only if the LNA terminal load equals the 50 Ω reference impedance Z_{ref}.

$$\vec{E}_{(\theta,\varphi,r,\omega)} = \frac{-j\eta\omega I_t}{4\pi c}\frac{e^{\frac{-j\omega r}{c}}}{r}\vec{H}^{ant}_{(\theta,\varphi,\omega)}\ ,\ with\ \eta = 377\Omega\ and\ c = 3.10^8\ ms^-1 \tag{3}$$

$$\vec{H}^{bfy}_{(\theta,\varphi,\omega)} = \frac{j4\pi c}{\eta I_t \omega}\vec{E}_{(\theta,\varphi,r,\omega)} r e^{\frac{j\omega r}{c}} \frac{S_{21}}{\frac{Z_{ant}}{Z_{ref}}(1-S_{11})+(1+S_{11})}\ ,\ with\ \vec{V}^{nec}_{(\theta,\varphi,\omega)} = \vec{E}_{(\theta,\varphi,r,\omega)} r e^{\frac{j\omega r}{c}} \tag{4}$$

We calculate the discrete Fourier transform of an input impulse $\vec{e}(\theta,\varphi,t)$ collinear to the antenna along the x-axis and without radial component, multiply it by $\vec{H}^{bfy}$, come back in the time domain and obtain the impulse induced voltage $s(t)$ at the LNA output. For a given $\vec{e}(t)$ filtered in a given bandwidth, we calculate the maximum of $|s(t)|$ and repeat it for every θ and φ direction to build a time domain isotropy pattern as shown on Fig. 3. This pattern has the advantage to use both magnitude and phase characteristics of the overall active antenna, which is much more convenient than the antenna gain when working in the time domain.

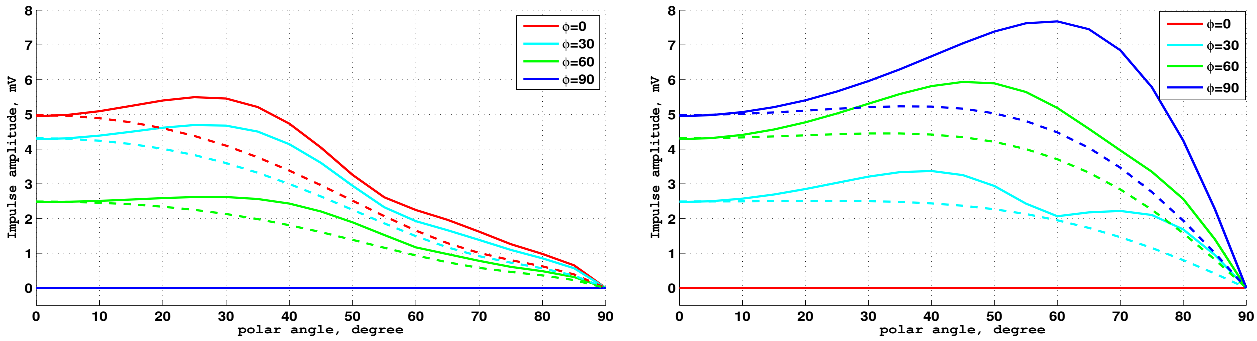

FIGURE 3. Time domain isotropy pattern of a 1.5 m height Butterfly antenna above a lossy average ground as a function of the polar angle and parametrized by the azimuth angle in degree. Butterfly-LONAMOS response to a 10-200 MHz bandwidth limited dirac pulse normalized to 1 mV.m^{-1} (full line). Similarly the same (dotted line) for a 20-80 MHz range (implies a 0.319 mV input impulse amplitude). Left figure is for the $\vec{e}_\theta$ direction and right for the $\vec{e}_\varphi$ direction.

CONCLUSION

A new antenna with three orthogonal polarizations using LONAMOS, and with a sensitivity, bandwidth, and phase distortion similar to the Butterfly antenna is under development. Adding a vertical polarisation will improve the sensitivity for high polar angles and ease the measurement of the electric field induced by UHECR in the three dimensions space.

REFERENCES

1. D. Charrier, *Nucl. Instr. and Meth. A* (2010), URL `http://dx.doi.org/10.1016/j.nima.2010.10.141`.
2. L. Martin, *Nucl. Instr. and Meth. A* (2013), URL `http://dx.doi.org/10.1016/j.nima.2013.12.024`.
3. C. Ballanis, *Antenna Theory*, Wiley, 2005, third edn.
4. H. Rothe, and W. Dahlke, "Theory of Noisy Fourpoles," in *Proc. of the IRE*, 1956, pp. 811–818.
5. H. et al., *PASP* (2012), URL `http://adsabs.harvard.edu/abs/2012PASP..124.1090H`.